

AperTO - Archivio Istituzionale Open Access dell'Università di Torino

## General retention parameters of chiral analytes in cyclodextrin gas chromatographic columns

### **This is the author's manuscript**

*Original Citation:*

*Availability:*

This version is available <http://hdl.handle.net/2318/148117> since 2015-12-22T13:24:45Z

*Published version:*

DOI:10.1016/j.chroma.2014.03.027

*Terms of use:*

Open Access

Anyone can freely access the full text of works made available as "Open Access". Works made available under a Creative Commons license can be used according to the terms and conditions of said license. Use of all other works requires consent of the right holder (author or publisher) if not exempted from copyright protection by the applicable law.

(Article begins on next page)



## UNIVERSITÀ DEGLI STUDI DI TORINO

This Accepted Author Manuscript (AAM) is copyrighted and published by Elsevier. It is posted here by agreement between Elsevier and the University of Turin. Changes resulting from the publishing process - such as editing, corrections, structural formatting, and other quality control mechanisms - may not be reflected in this version of the text. The definitive version of the text was subsequently published in [*Journal of Chromatography A*, Volume: 1340, Pages: 121-127, date: MAY 2 2014, DOI: <http://dx.doi.org/10.1016/j.chroma.2014.03.027>].

You may download, copy and otherwise use the AAM for non-commercial purposes provided that your license is limited by the following restrictions:

- (1) You may use this AAM for non-commercial purposes only under the terms of the CC-BY-NC-ND license.
- (2) The integrity of the work and identification of the author, copyright owner, and publisher must be preserved in any copy.
- (3) You must attribute this AAM in the following format: Creative Commons BY-NC-ND license (<http://creativecommons.org/licenses/by-nc-nd/4.0/deed.en>), <http://dx.doi.org/10.1016/j.chroma.2014.03.027>

1 **General retention parameters of chiral analytes in cyclodextrin gas**  
2 **chromatographic columns**

---

3

4 Carlo Bicchi<sup>1</sup>, Leonid Blumberg<sup>2</sup>, Patrizia Rubiolo<sup>1</sup>, Cecilia Cagliero<sup>1</sup>

5 <sup>1</sup>Dipartimento di Scienza e Tecnologia del Farmaco, Facoltà di Farmacia, Università degli Studi di  
6 Torino, Via Pietro Giuria 9, Turin 10125, Italy.

7  
8 <sup>2</sup>Fast GC Consulting, P.O. Box 1423, Wilmington, DE 19801, USA

9

10 Address for correspondence:

11 Prof. Dr. Carlo Bicchi

12 Dipartimento di Scienza e Tecnologia del Farmaco, Facoltà di Farmacia, Università degli Studi di  
13 Torino, Via Pietro Giuria 9, Turin 10125, Italy.

14 Tel +39 0116707662; fax: +39 0116707687; e-mail: carlo.bicchi@unito.it

15

16 **Abstract**

17 Two thermodynamic parameters – entropy ( $\Delta S$ ) and enthalpy ( $\Delta H$ ) – ideally describe the  
18 thermodynamics of how the retention of an analyte in a stationary phase depends on the temperature.  
19 The paper examines the conversion of an analyte's entropy and enthalpy into chromatographically more  
20 meaningful equivalents: its characteristic temperature and thermal constant. Thermodynamic and  
21 characteristic parameters of 29 enantiomer pairs of chiral analytes, analysed with four cyclodextrin  
22 stationary phases, were measured, tabulated, and investigated. The distribution of all newly-measured  
23 characteristic parameters was found to be similar to the known distribution of these parameters for some  
24 12,000 pairs of analytes, analysed with several stationary phases. This similarity suggests that the peak  
25 widths of the investigated analytes in temperature-programmed analyses should be generally the same as  
26 the peak widths of other similarly retained analytes. It also suggests that the previously-known optimum  
27 general heating rate (about  $10^\circ\text{C}/t_M$ , i.e.  $10^\circ\text{C}$  per hold-up time) is also the general optimum for  
28 temperature-programmed enantioselective GC analyses with cyclodextrins as stationary phases.

29 The optimum general heating rate corresponds to the shortest analysis time for a predetermined peak  
30 capacity. It can substantially differ from specific optima corresponding to the best separation of  
31 particular peak pairs. Theoretical prediction of these specific optima requires more complex non-ideal  
32 thermodynamic models, and more accurate measurement of the parameters involved – these topics that  
33 are outside the scope of this report.

34

35 **Keywords:** characteristic temperature, characteristic thermal constant, optimal heating rate,  
36 enantioselective gas chromatography, cyclodextrin stationary phases

## 37 1 Introduction

38 An *ideal thermodynamic model* of the distribution of an analyte between stationary and mobile  
39 phases in a column describes the analyte's *distribution constant* ( $K_c$ ) as [1]

$$40 \ln K_c = -\frac{\Delta S}{R} + \frac{\Delta H}{RT} \quad (1)$$

41 where  $R \approx 8.3145$  J/K/mol is the *molar gas constant*,  $T$  is the column (absolute) *temperature*, and  $\Delta S$   
42 and  $\Delta H$  are the *entropy* and *enthalpy* of the distribution.

43 The ideal thermodynamic model in Eq. (1) is not sufficiently accurate for prediction of peak  
44 retention times and separations, and of other chromatographic details. More accurate (and more  
45 complex) models are needed to predict these specifics [2-7]. However, Eq. (1) adequately describes the  
46 *general thermodynamic properties*, which are sufficient to evaluate some *general performance*  
47 *characteristics* of isothermal and temperature-programmed analyses, including analysis times, peak  
48 widths, and peak capacities [8-10]. In addition, the accuracy requirements for measuring parameters to  
49 evaluate general performance characteristics of GC analyses are less stringent than those required for  
50 more specific predictions.

51 This report studies the general retention properties of chiral analytes in chiral recognition, with four  
52 cyclodextrin stationary phases coated on open-tubular (*capillary*) columns [11]. Thermodynamic  
53 parameters  $\Delta S$  and  $\Delta H$  provide sufficient information for these studies, although they present substantial  
54 shortcomings. They do not offer a direct and intuitive representation of the analyte's elution parameters,  
55 nor of the corresponding peaks' parameters. These properties of an analyte are more directly and  
56 intuitively represented by its characteristic temperature ( $T_{\text{char}}$ ) and characteristic thermal constant ( $\theta_{\text{char}}$ )  
57 [8, 12]. The former is the temperature at which the analyte retention factor ( $k$ ) is equal to one; the latter  
58 is the negative of the inverse of the slope of the function  $\ln k(T)$ . Parameters  $T_{\text{char}}$  and  $\theta_{\text{char}}$  have several  
59 useful properties.  $T_{\text{char}}$  is close to the elution temperature of the analyte in a typical temperature-

60 programmed analysis. This makes  $T_{\text{char}}$  a good indicator of the elution order of enantiomer pairs.  $\theta_{\text{char}}$   
61 directly affects the peak widths, and is proportional to the optimal heating rate corresponding to the best  
62 trade-off between peak capacity and analysis time in a temperature-programmed GC analysis [9, 10, 12,  
63 13].

64 In our previous study [14], we found that the heating rates ( $R_{\text{T,chiral}}$ ) providing acceptable separation  
65 of the target enantiomer pairs in the shortest time were several times lower than general optimal heating  
66 rate ( $R_{\text{T,Opt}}$ , 10°C per hold-up time [9, 13]) corresponding to the shortest analysis time for a given peak  
67 capacity. Possible explanations could be: i) the characteristic thermal constants ( $\theta_{\text{char}}$ ) of the investigated  
68 analytes [14] were proportionally lower compared to previously known  $\theta_{\text{char}}$  of thousands of other  
69 analytes [8, 10]; ii) the separation of closely spaced enantiomer pairs substantially depends on the  
70 difference in their  $\theta_{\text{char}}$  [8] while the general optimal heating rate only depends on the average value of  
71  $\theta_{\text{char}}$  for all analytes in a given analysis, and not on the difference between  $\theta_{\text{char}}$  of specific analytes [9,  
72 13]. These reasons can be sorted out by measurement of thermodynamic parameters of enantiomer pairs.  
73 This study is divided into two stages. This report is the first stage aimed to measure the thermodynamic  
74 and characteristic parameters of the target analytes and to find if there is a meaningful difference  
75 between the newly found values of  $\theta_{\text{char}}$  and their known counterparts for thousands of other analytes.  
76 As shown below, such difference does not exist. This opens the way and provides justification for the  
77 next more detailed and more time-consuming measurements targeting evaluation of the differences  
78 between  $\theta_{\text{char}}$  of enantiomer pairs. This investigation is under way.

79 This paper reports the thermodynamic and characteristic parameters of 29 chiral enantiomer pairs,  
80 analysed in four cyclodextrin stationary phases, together with the optimal heating rates corresponding to  
81 the best trade-off between the peak capacity and analysis time in temperature-programmed chiral  
82 analyses [9, 13]. Unless otherwise is explicitly stated, all temperatures ( $T$ ) in this report are in kelvins.

## 83 2 Theory

### 84 2.1 Characteristic retention parameters of analytes

85 It follows from Eq. (1) that the temperature-dependence,  $k(T)$ , of the *retention factor* ( $k$ ) of an  
86 analyte in a wall-coated open-tubular (*capillary*) column, with *internal diameter*  $d_c$  and stationary phase  
87 *film thickness*  $d_f$ , can be described as [8]

$$88 \ln k = \ln k(T) = \ln(4\varphi) - \frac{\Delta S}{R} + \frac{\Delta H}{RT} \quad (2)$$

89 where  $R \approx 8.3145 \text{ J/K/mol}$  is the molar gas constant,  $\Delta S$  and  $\Delta H$  are the entropy and enthalpy of  
90 evaporation of the analyte from the stationary phase, and  $\varphi$  is the *relative film thickness*, defined as [8]

$$91 \varphi = \frac{V_f}{4V_g} = \frac{1}{4\beta} \quad (3)$$

92 where  $V_f$ ,  $V_g$ , and  $\beta$  are, respectively, the volume of the stationary phase film, the volume of the gas, and  
93 the *phase ratio* in the column. The advantages of  $\varphi$  over  $\beta$  have been discussed elsewhere [8]. Typically,  
94  $d_f$  is much smaller than  $d_c$ , i.e.  $d_f \ll d_c$ ; in this case,  $\varphi$  can be approximated as  $\varphi \approx d_f/d_c$ . This report  
95 will assume that

$$96 \varphi = \frac{d_f}{d_c} \quad (4)$$

97 The function  $k(T)$  in Eq. (2) depends on four parameters:  $R$ ,  $\varphi$ ,  $\Delta S$  and  $\Delta H$ . Only the last two ( $\Delta S$  and  
98  $\Delta H$ ) may differ for different analytes in a single stationary phase; of the two others,  $R$  is the universal  
99 constant, and  $\varphi$  is a column parameter that is the same for all analytes. The thermodynamic parameters  
100  $\Delta S$  and  $\Delta H$  of an analyte provide a straightforward description of the thermodynamics of its interaction  
101 with the stationary phase, but do not offer a direct representation of chromatographic parameters of the  
102 analyte and of the corresponding peak. Consider, for example, an analyte with  $\Delta S = 70 \text{ J/mol/K}$  and  
103  $\Delta H = 50 \text{ kJ/mol}$ . What would be its elution temperature in a typical temperature-programmed analysis?

104 What should be the temperature change in isothermal analysis e. g. in order to double the analytes'  
 105 retention factor? The answers to these questions could be found from  $\Delta H$  and  $\Delta S$  parameters, although  
 106 not directly. Chromatographically meaningful parameters that directly answer these and similar  
 107 chromatographic questions can be found from reducing the number of parameters in Eq. (2) from the  
 108 total of four ( $R$ ,  $\varphi$ ,  $\Delta S$  and  $\Delta H$ ) to the minimum of two mutually independent parameters. Such  
 109 modification of Eq. (2) can be expressed as [8-10]:

$$110 \quad \ln k = \ln k(T) = \frac{T_{\text{char}}}{\theta_{\text{char}}} \left( \frac{T_{\text{char}}}{T} - 1 \right) \quad (5)$$

111 where  $T_{\text{char}}$  and  $\theta_{\text{char}}$  are, respectively, the *characteristic temperature* and *characteristic thermal*  
 112 *constant* [8-10, 12] of retention of a given analyte in a given column. The key properties of these  
 113 parameters will be examined after describing their relationship to parameters  $\Delta S$  and  $\Delta H$ .

114 The pair  $\Delta S$  and  $\Delta H$  can be transformed into the pair  $T_{\text{char}}$  and  $\theta_{\text{char}}$ , and vice versa, through the  
 115 following equations (Eqs. (6) and (7)) which are obtained by solving together Eqs. (2) and (5) at an  
 116 arbitrary  $T$  and at  $T = T_{\text{char}}$  [9, 10]:

$$117 \quad T_{\text{char}} = \frac{\Delta H}{\Delta S - R \ln(4\varphi)}, \quad \theta_{\text{char}} = \frac{R \Delta H}{(\Delta S - R \ln(4\varphi))^2} \quad (6)$$

$$118 \quad \Delta S = R \left( \frac{T_{\text{char}}}{\theta_{\text{char}}} + \ln(4\varphi) \right), \quad \Delta H = \frac{R T_{\text{char}}^2}{\theta_{\text{char}}} \quad (7)$$

119 Eq. (6) shows that the characteristic parameters ( $T_{\text{char}}$  and  $\theta_{\text{char}}$ ) depend on the relative film thickness  
 120 ( $\varphi$ ). Assume that the parameters  $T_{\text{char}1}$  and  $\theta_{\text{char}1}$  corresponding to  $\varphi_1$  are known, it follows directly from  
 121 Eqs. (6) and (7) that if parameters  $T_{\text{char}1}$  and  $\theta_{\text{char}1}$  at  $\varphi_1$  are known then parameters  $T_{\text{char}2}$  and  $\theta_{\text{char}2}$  at  $\varphi_2$   
 122 can be found as

$$123 \quad T_{\text{char}2} = \frac{T_{\text{char}1}^2}{T_{\text{char}1} + \theta_{\text{char}1} \ln(\varphi_1/\varphi_2)} \quad (8)$$



124 
$$\theta_{\text{char}2} = \frac{T_{\text{char}1}^2 \theta_{\text{char}1}}{\left(T_{\text{char}1} + \theta_{\text{char}1} \ln(\varphi_1/\varphi_2)\right)^2} \quad (9)$$

125 *2.1.1 Chromatographic properties of characteristic parameters  $T_{\text{char}}$  and  $\theta_{\text{char}}$*

126 From the mathematical standpoint, the  $T_{\text{char}}$  of an analyte is the  $T$ -intercept (Figure 1) of the function  
 127  $\ln k(T)$  for the analyte: at  $T = T_{\text{char}}$ , Eq. (5) yields  $\ln k = 0$ .  $\theta_{\text{char}}$  is the negative (multiplied by -1) of the  
 128 inverse of the slope of  $\ln k(T)$  at its  $T$ -intercept (Figure 1): differentiation of the right hand side of Eq.  
 129 (5) yields the following expression for the negative of the inverse of the slope,  $d \ln k(T) / dT$ , of  
 130  $\ln k(T)$  at  $T = T_{\text{char}}$ :

131 
$$-\left(\frac{d \ln k}{dT}\right)^{-1} = -\left(\frac{T_{\text{char}}}{\theta_{\text{char}}} \frac{d}{dT} \left(\frac{T_{\text{char}}}{T} - 1\right)\right)^{-1} = \frac{T^2 \theta_{\text{char}}}{T_{\text{char}}^2} = \theta_{\text{char}} \quad (10)$$

132 The reason why the negative and inversion of the slope of  $\ln k(T)$  are adopted in defining  $\theta_{\text{char}}$  stems  
 133 from the following considerations. An increase in column temperature ( $T$ ) reduces the analyte retention  
 134 factor ( $k$ ); as a result, the function  $\ln k(T)$  has a negative slope. Taking its negative conveniently makes  
 135  $\theta_{\text{char}}$  into a positive quantity. Furthermore, the slope of  $\ln k(T)$  is measured in inverse temperature units  
 136 (e.g. 1/K or 1/°C). Inverting the slope, as in  $\theta_{\text{char}}$ , gives a quantity that is measured in the more  
 137 convenient units of temperature. This approach has the advantage of expressing both the temperature  
 138 ranges of heating ramps, and the ranges of characteristic temperatures, in units of  $\theta_{\text{char}}$  [8-10, 12]. Thus,  
 139 since the typical value of  $\theta_{\text{char}}$  is about 30°C [8, 10, 15] (see also below), it may be said that a heating  
 140 ramp from 50°C to 260°C covers the temperature range of approximately 7 characteristic temperatures.  
 141 This and similar assessments have important fundamental implications regarding the peak capacity of  
 142 temperature-programmed GC analyses [10].

143 Since  $\theta_{\text{char}}$  is the inversion of the slope of  $\ln k(T)$ , it may be viewed as its *anti-slope* – a measure of  
 144 the *insensitivity* of the retention factor ( $k$ ) to changes in column temperature ( $T$ ). The larger is  $\theta_{\text{char}}$ , the

145 larger must the change in  $T$  be to produce the same change in  $k$ . The average value of characteristic  
146 thermal constants ( $\theta_{\text{char}}$ ) is approximately 30°C, suggesting that a temperature increase of 30° should  
147 cause about an  $e$ -fold reduction in  $k$  ( $e \approx 2.72$ , the base of natural logarithms); approximately a 20°C  
148 ( $\theta_{\text{char}} \ln 2$ ) temperature increase is required to reduce  $k$  by a factor of two; a 1°C increase in column  
149 temperature causes about a 3.3% ( $1/\theta_{\text{char}} \approx 0.033/\text{K}$ ) reduction in  $k$ . These theoretical observations [8]  
150 are supported by experimental results [16-18].

151 The characteristic temperature ( $T_{\text{char}}$ ) also has direct chromatographic interpretation: as was already  
152 mentioned, at  $T = T_{\text{char}}$ , Eq. (5) yields  $\ln k = 0$ , i.e.  $k = 1$ . In a single-ramp temperature-programmed  
153 analysis, all analytes elute with approximately the same retention factor [8, 12], and the elution  
154 temperature of each solute is close to its  $T_{\text{char}}$ . In particular, an analyte eluting in a temperature-  
155 programmed analysis at its own characteristic temperature elutes with a retention factor of one.  
156 Typically, the *elution temperature* ( $T_{\text{R}}$ ) of an analyte in a temperature-programmed analysis may differ  
157 from  $T_{\text{char}}$ , but will closely approximate to it [8, 9, 12]. The  $T_{\text{char}}$  of an analyte can therefore be viewed  
158 as its approximate elution temperature in a typical temperature-programmed analysis. As a result, from a  
159 knowledge of the characteristic temperature ( $T_{\text{char}}$ ) of an analyte, its elution temperature can be  
160 estimated and, in consequence, other temperature-dependent parameters. These include the diffusivities  
161 of the eluting analytes in temperature-programmed analysis, the optimal carrier gas flow rate, and the  
162 viscosity at the time of the analyte elution. [8]. Taking the case, considered above, of an analyte having  
163  $\Delta H = 50 \text{ kJ/mol}$  and  $\Delta S = 70 \text{ J/mol/K}$ : these data provide little direct chromatographic information.  
164 However, they can be transformed into  $\theta_{\text{char}}$ . For a column with  $\varphi = 0.001$  (Figure 1),  $T_{\text{char}}$  is 431K  
165 ( $\approx 158^\circ\text{C}$ ) and  $\theta_{\text{char}}$  is 31°C. This indicates that, in a typical temperature-programmed GC analysis, the  
166 analyte elution temperature is close to 160°C, and the column temperature should be reduced by about  
167 21.5°C ( $31 \cdot \ln 2 \approx 21.5$ ) in order to double the analyte retention factor in isothermal analysis,

168 An important property of  $\theta_{\text{char}}$  is that the optimal heating rate in temperature-programmed GC is a  
 169 direct function of parameters  $\theta_{\text{char}}$  for all analytes in the sample [9, 13]. Each analyte in the sample has  
 170 its own value of  $T_{\text{char}}$  and  $\theta_{\text{char}}$ . However, the general trend is that the analytes with higher  $T_{\text{char}}$  values  
 171 tend also to have higher  $\theta_{\text{char}}$  values [8, 10]. This means that the retention factors of later-eluting  
 172 analytes tend to be less sensitive to temperature change than are the retention factors of earlier-eluting  
 173 ones. The characteristic parameters also depend on film thickness, as is shown in Eqs. (8) and (9); this  
 174 dependency can be described by a simpler approximation, which is sufficiently accurate for the purpose  
 175 of general evaluation [8]. On the basis of a study carried out on a large number of analytes (more than  
 176 12,000 analyte-phase pairs [8, 10]) with about 60 different stationary phases, the general trend of the  
 177 dependence of  $\theta_{\text{char}}$  on  $T_{\text{char}}$ , in a column with relative film thickness  $\varphi$ , can be described as (see also  
 178 Figure 2)

$$179 \quad \theta_{\text{char}} = \left( \frac{T_{\text{char}}}{T_{\text{st}}} \right)^{0.7} \theta_{\text{char,st}}, \quad \theta_{\text{char,st}} = (10^3 \varphi)^{0.09} 22^\circ \text{C} \quad (11)$$

180 where  $T_{\text{st}} = 273.15 \text{ K}$  ( $0^\circ \text{C}$ ) is the *standard temperature*. Eq. (11) shows that an increase in the relative  
 181 film thickness ( $\varphi$ ) tends to produce an increase in  $\theta_{\text{char}}$  for a given  $T_{\text{char}}$ , although the dependence of  $\theta_{\text{char}}$   
 182 on  $\varphi$  is rather weak. Thus a 10-fold increase in  $\varphi$  causes about a 23% increase in  $\theta_{\text{char}}$  at a given  $T_{\text{char}}$ .  
 183 For each  $T_{\text{char}}$ , the  $\theta_{\text{char}}$  values of a large majority of the earlier investigated analytes [8, 10] lie within  
 184  $\pm 10^\circ \text{C}$  of the values found from Eq. (11).

185 Other properties of the characteristic parameters  $T_{\text{char}}$  and  $\theta_{\text{char}}$ , including additional details of their  
 186 dependence on film thickness, have been described elsewhere [8, 12].

## 187 3 Experimental

### 188 3.1 Samples

189 Pure standards of the analytes investigated were from the collection in the authors' laboratory. All  
190 standard compounds were solubilised in cyclohexane at a concentration of 100 ppm mg/L each. Solvents  
191 were all HPLC grade from Riedel-de Haen (Seelze, Germany). Table 1 reports the list of the analytes  
192 investigated in this study.

193 [*Please insert Table 1 here*]

194

### 195 3.2 Columns

196 The analyses were carried out on 25m×0.25mm×0.25µm ( $L \times d_c \times d_f$ ) columns from Mega (Legnano –  
197 Italy) coated with the following cyclodextrin derivatives:

198 6<sup>I-VII</sup>-*O*-TBDMS-2<sup>I-VII</sup>-3<sup>I-VII</sup>-*O*-acetyl-β-CD (DA)

199 6<sup>I-VII</sup>-*O*-TBDMS-2<sup>I-VII</sup>-3<sup>I-VII</sup>-*O*-ethyl-β-CD (DE)

200 6<sup>I-VII</sup>-*O*-TBDMS-2<sup>I-VII</sup>-3<sup>I-VII</sup>-*O*-methyl-β-CD (DM)

201 3<sup>I-VII</sup>-*O*-pentyl-2<sup>I-VII</sup>-6<sup>I-VII</sup>-*O*-methyl-β-CD (PEN)

202 Each cyclodextrin derivative was at a concentration of 30% in PS086 as diluting stationary phase.

### 203 3.3 Instruments

204 Analyses were carried out on a Shimadzu GC 2010 system (Shimadzu, Milan, Italy) provided with  
205 an FID; data were processed with Shimadzu GC Solution 2.53SU1 software.

### 206 3.4 GC conditions

207 The retention parameters of all analytes in all columns were found from isothermal analyses at the  
208 following temperatures: 50, 75, 100, 125, 150, 175, 200, 210, 220, and 230°C. Carrier gas was helium at  
209 1 mL/min flow rate. Injector and detector temperatures were 220°C and 230°C, respectively.

## 210 4 Results and discussion

211 The values of the thermodynamic ( $\Delta S$  and  $\Delta H$ ) and characteristic ( $T_{\text{char}}$  and  $\theta_{\text{char}}$ ) retention  
212 parameters for the analytes listed in Table 1 are summarized in Table 2.

213 [*Please insert Table 2 here*]

214

215 The dimensionless film thickness ( $\phi$ ) in the investigated column was 0.001. Figure 3 shows the  
216 distribution maps of the ( $T_{\text{char}}$ ,  $\theta_{\text{char}}$ )-points for each stationary phase, and Figure 4 shows the combined  
217 distribution map. The least-square fit of the line  $AT^{0.7}$  for the combined data can be expressed as

$$218 \theta_{\text{char}} = \theta_{\text{char,st}} \left( \frac{T_{\text{char}}}{T_{\text{st}}} \right)^{0.7}, \quad \theta_{\text{char,st}} = 18^\circ \text{C} \quad (12)$$

219 The difference between this line and that for the other analytes and stationary phases in Eq. (11) is only  
220 in the scale.  $\theta_{\text{char}}$  for the analytes investigated in this report are generally about 18% lower compared to  
221 the ones in Eq. (11). As a result, the peak widths in temperature-programmed analyses of chiral analytes  
222 investigated here should be practically the same as the peak widths of other analytes under the same  
223 conditions.

224 An important property of characteristic thermal constants ( $\theta_{\text{char}}$ ) of the analytes in a sample analyzed  
225 by a column is that the optimal heating rate ( $R_{\text{T,Opt}}$ ) corresponding to the best separation-time trade-off is  
226 a direct function of the distribution (Figure 2 or Figure 4) of quantities  $\theta_{\text{char}}$  [9, 13]. The best separation-  
227 time trade-off means here to obtain the shortest analysis time at a given peak capacity or, conversely, the

228 largest peak capacity at a given analysis time. The numerical value of  $R_{T,Opt}$  significantly depends on  
229 column dimensions, carrier gas type, flow rate, and other conditions. For example,  $R_{T,Opt}$  for a  
230 10m×0.25mm column in GC-MS is much higher than for a 100m×0.25mm column. However, there is a  
231 metric that uniquely expresses  $R_{T,Opt}$  for different columns under various chromatographic conditions.  
232 This is the *normalized heating rate* defined as the product  $R_T t_M$  which is measured in units of  
233 temperature and describes  $R_T$  in terms of the temperature change during the time span equal to  $t_M$  [8-10,  
234 13, 19]. The *optimal normalized heating rate* ( $R_{T,Opt} t_M$ ) is proportional to the scale factor ( $\theta_{char,st}$ ) in  
235 Eqs. (11) and (12) describing the distribution (Figure 2 or Figure 4) of  $\theta_{char}$  [9, 12, 13].  $R_{T,Opt} t_M$  also  
236 slightly depends on the dimensionless film thickness ( $\varphi$ ).

237 At  $\varphi = 0.001$  in Eq. (11),  $\theta_{char,st}$  is equal to 22°C. For this condition,  $R_{T,Opt} t_M$  in isobaric analyses  
238 should be approximately  $10^\circ\text{C}/t_M$  (10°C per hold-up time) [9, 13]. Eq. (11) and, therefore, the result of  
239  $R_{T,Opt} \approx 10^\circ\text{C}/t_M$  are valid for all previously evaluated distributions of  $\theta_{char}$  illustrated in Figure 2. On  
240 the other hand, in the  $\theta_{char}$ -distribution for 29 enantiomer pairs in four cyclodextrin phases evaluated  
241 here,  $\theta_{char,st} = 18^\circ\text{C}$  (Eq. (12), Figure 4), i.e. 18% lower than  $\theta_{char,st}$  in Eq. (12). This suggests that  $R_{T,Opt}$   
242 for the columns and analytes investigated in this report should be about 18% lower than  $R_{T,Opt}$  for the  
243 majority of other analyses. Thus, the general recommendation, to use  $10^\circ\text{C}/t_M$  in isobaric temperature-  
244 programmed analyses [9, 13], should be reduced to  $8^\circ\text{C}/t_M$  for the chiral stationary phases and analytes  
245 investigated here. In our view explained below, this difference is insignificant, and may be disregarded  
246 in practice. [9, 13].

247 The following factors should also be considered [9, 13].

- 248 • The optimum heating rate depends on the pressure conditions in the column. The optimum is  
249 typically close to  $10^\circ\text{C}/t_M$  when gas decompression along the column is strong, and the GC  
250 instrument is capable of providing the required pressure. These conditions are typical for all GC-

251 MS analyses (vacuum at the column outlet), and for analyses of complex mixture requiring  
252 relatively long and narrow-bore columns. The  $8^{\circ}\text{C}/t_{\text{M}}$  is optimal for these conditions when  
253 cyclodextrin stationary phases are used for GC chiral recognition. Relatively short wide-bore  
254 columns with atmospheric pressure at the outlet are typically used to analyse relatively simple  
255 mixtures; these analyses do not always require temperature programming, but if they do, the  
256 optimum heating rate is about  $15^{\circ}\text{C}/t_{\text{M}}$ . In some relatively rare cases, heating rate optimization  
257 can only be achieved at the maximum pressure available from the GC instrument; under these  
258 conditions, the optimum heating rate is close to  $7.5^{\circ}\text{C}/t_{\text{M}}$ .

- 259 • Theoretical and experimental graphs describing the quantitative dependence of the  
260 separation/time trade-off on the heating rate suggest that, in the vicinity of its optimal value, the  
261 normalized heating rate causes relatively small changes in analysis time at a given peak capacity.  
262 Thus, increasing the normalized heating rate to 50% above its optimum value requires less than  
263 10% increase in analysis time, to maintain a peak capacity constant. An increase of the  
264 normalized heating rate to 20% above its optimum value causes a peak capacity reduction that is  
265 insignificant in practical terms . This suggests that the difference between  $10^{\circ}\text{C}/t_{\text{M}}$  and  $8^{\circ}\text{C}/t_{\text{M}}$  is  
266 insignificant in practice.
- 267 • Real-world samples contain additional components other than those investigated here. The  
268 optimum heating rate to analyse such mixtures on cyclodextrin columns is likely to be  
269 somewhere between  $10^{\circ}\text{C}/t_{\text{M}}$  and  $8^{\circ}\text{C}/t_{\text{M}}$ .

270 These observations suggest that  $10^{\circ}\text{C}/t_{\text{M}}$  is appropriate as a single practical recommendation for a  
271 default heating rate in all temperature-programmed GC analyses, including analysis of chiral analytes  
272 with cyclodextrins.

273 In a previous study [14], we found that the heating rates ( $R_{\text{T,chiral}}$ ) providing acceptable separation of  
274 the target enantiomer pairs in the shortest time were several times lower than  $R_{\text{T,Opt}}$  of  $10^{\circ}\text{C}/t_{\text{M}}$ . Since

275  $\theta_{\text{char}}$  and  $R_{T,\text{Opt}}$  for the chiral analytes investigated here are about the same as their counterparts for all  
276 other previously evaluated analytes and stationary phase pairs [9, 13], the substantial departure of  
277  $R_{T,\text{chiral}}$  from  $10^\circ\text{C}/t_{\text{M}}$  can only be explained by the difference in  $\theta_{\text{char}}$  of the enantiomers [8] rather than  
278 by the absolute values of their  $\theta_{\text{char}}$ .

279 The differences in enantiomer pairs' characteristic parameters and their effect on optimal conditions  
280 for the separation of specific pairs will be the subject of a forthcoming publication.

## 281 5 Conclusions

282 The transformation of entropy ( $\Delta S$ ) and enthalpy ( $\Delta H$ ) of distribution of analyte between the  
283 stationary and the mobile phases in a wall-coated open tubular column, into the more  
284 chromatographically-meaningful characteristic temperature ( $T_{\text{char}}$ ) and characteristic thermal constant  
285 ( $\theta_{\text{char}}$ ) was examined, together with the inverse transformation of  $T_{\text{char}}$  and  $\theta_{\text{char}}$  into  $\Delta S$  and  $\Delta H$ . The  
286 physical meaning of the characteristic parameters ( $T_{\text{char}}$  and  $\theta_{\text{char}}$ ) of analyte retention, and their  
287 advantages over their thermodynamic counterparts ( $\Delta S$  and  $\Delta H$ ), were discussed. All these parameters  
288 ( $\Delta S$ ,  $\Delta H$ ,  $T_{\text{char}}$ ,  $\theta_{\text{char}}$ ) were measured experimentally and tabulated for 29 chiral pairs of analytes, in four  
289 different cyclodextrin stationary phases, for a total of 232 analyte/phase pairs. The distribution maps of  
290 ( $T_{\text{char}}$ ,  $\theta_{\text{char}}$ )-points for these 232 analyte-phase pairs were similar to those for some 12,000 previously  
291 investigated analyte-phase pairs for about 60 different stationary phases. This similarity implies that the  
292 general optimal heating rate, corresponding to the best trade-off between peak capacity and analysis  
293 time, in temperature-programmed chiral analyses with cyclodextrins as stationary phases, is  
294 approximately the same as that for conventional GC analyses (about  $10^\circ\text{C}/t_{\text{M}}$ , i.e.  $10^\circ\text{C}$  per hold-up  
295 time). The optimal heating rates, corresponding to the best performance in terms of separation of  
296 specific peak pairs, may differ substantially from the general optimum of  $10^\circ\text{C}/t_{\text{M}}$ , and deserve a special  
297 study.



298 **Acknowledgements**

299 The authors are indebted with the project: “Progetti di Ricerca finanziati dall’Università degli Studi di  
300 Torino (ex 60%) – Anno 2012”.

301 **6 List of the acronyms**

Symbol	Description
$d_c$	column internal diameter
$d_f$	stationary phase film thickness
$\Delta H$	enthalpy of evaporation
$k$	retention factor
$K_c$	distribution constant, Eq. (1)
$R$	molar gas constant, $R \approx 8.3145 \text{ J/K/mol}$
$\Delta S$	entropy of evaporation
$T$	temperature
$T_{\text{char}}$	characteristic temperature, Eq. (6)
$T_{\text{st}}$	standard temperature, $T_{\text{st}} = 273.15 \text{ K}$
$t$	time
$t_M$	hold-up time
$\theta_{\text{char}}$	characteristic thermal constant, Eq. (6)
$\theta_{\text{char,st}}$	characteristic thermal constant at $T_{\text{char}} = T_{\text{st}}$ in Eq. (11)
$\varphi$	relative film thickness, Eq. (4)

302

303

304 **7 References**

- 305 [1] J. C. Giddings, *Unified Separation Science*, Wiley, New York, 1991.
- 306 [2] R. C. Castells, E. L. Arancibia, A. M. Nardillo, *J. Chromatogr.* 504 (1990) 45.
- 307 [3] S. Vezzani, P. Moretti, G. Castello, *J. Chromatogr.* 677 (1994) 331.
- 308 [4] F. R. González, *J. Chromatogr. A* 942 (2002) 211.
- 309 [5] K. Aryasuk, K. Krisnangkura, *J. Sep. Sci.* 26 (2003) 1688.
- 310 [6] F. Aldaeus, Y. Thewalim, A. Colmsjö, *Anal. Bioanal. Chem.* 389 (2007) 941.
- 311 [7] B. Karolat, J. Harynuk, *J. Chromatogr. A* 1217 (2010) 4862.
- 312 [8] L. M. Blumberg, *Temperature-Programmed Gas Chromatography*, Wiley-VCH, Weinheim,  
313 2010.
- 314 [9] L. M. Blumberg, in C. F. Poole (Ed.), *Gas Chromatography*. Elsevier, Amsterdam, 2012, p. 19.
- 315 [10] L. M. Blumberg, *J. Chromatogr. A* 1244 (2012) 148.
- 316 [11] V. Schurig, *J. Chromatogr. A* 906 (2001) 275.
- 317 [12] L. M. Blumberg, M. S. Klee, *Anal. Chem.* 72 (2000) 4080.
- 318 [13] L. M. Blumberg, M. S. Klee, *J. Microcolumn Sep.* 12 (2000) 508.
- 319 [14] C. Bicchi, L. M. Blumberg, C. Cagliero, C. Cordero, P. Rubiolo, E. Liberto, *J. Chromatogr. A*  
320 1217 (2010) 1530.
- 321 [15] L. M. Blumberg, M. S. Klee, *Anal. Chem.* 73 (2001) 684.
- 322 [16] J. C. Giddings, *J. Chem. Educ.* 39 (1962) 569.
- 323 [17] E. Grushka, *Anal. Chem.* 42 (1970) 1142.
- 324 [18] A. B. Fialkov, A. Gordin, A. Amirav, *J. Chromatogr. A* 991 (2003) 217.
- 325 [19] L. M. Blumberg, M. S. Klee, *Anal. Chem.* 70 (1998) 3828.

326  
327

328

329 **Table headings**

330 Table 1. Standard racemates of 29 analytes of natural origin, having different chemical structures and  
331 volatilities (for a total of 58 analytes) investigated in this study. The analytes were diluted in  
332 cyclohexane at a concentration of 100ppm.

333

334 Table 2. Thermodynamic ( $\Delta S$ ,  $\Delta H$ ) and characteristic ( $T_{\text{char}}$ ,  $\theta_{\text{char}}$ ) retention parameters of the analytes  
335 listed in Table 1.

336

337

338 **Figure Captions**

339 Figure 1. Graph of the function  $\ln k(T)$ , Eq. (2), (solid line) for  $\varphi = 0.001$ ,  $\Delta H = 50000$  J/mol and  
340  $\Delta S = 70$  J/mol/K. The dashed line is the tangent to  $\ln k(T)$  at  $\ln k = 0$ , and thus at  $T = T_{\text{char}}$ .

341 Figure 2. Map of  $(T_{\text{char}}, \theta_{\text{char}})$ -points for more than 12,000 solute-liquid combinations involving capillary  
342 columns with more than 50 liquid stationary phases. There are more than 12,000 dots on the map. Each  
343 dot represents one solute (analyte) in one liquid polymer stationary phase at  $\varphi = 0.001$  [8, 10]. The  
344 dashed line represents Eq. (11) at  $\varphi = 0.001$ .

345 Figure 3. Distribution maps of  $(T_{\text{char}}, \theta_{\text{char}})$ -points for the analytes in Table 1; based on the data in Table  
346 2.

347 Figure 4. Combined distribution map of  $(T_{\text{char}}, \theta_{\text{char}})$ -points for the analytes in Table 1 on all four  
348 investigated columns; based on the data in Table 2. The solid and dashed lines are the graphs of  
349 equations Eq. (12) and Eq. (11) at  $\varphi = 0.001$ .

350

351 **Tables**

352 Table 1

#	Analyte	#	Analyte	#	Analyte
1	2-methylbutanol (R)	21	$\alpha$ pinene(S)	41	$\delta$ -undecalactone (X)
2	2-methylbutanol (S)	22	$\alpha$ pinene (R)	42	$\delta$ -undecalactone (Y)
3	2-octanol (X)	23	limonene (S)	43	$\delta$ -dodecalactone (X)
4	2-octanol (Y)	24	limonene (R)	44	$\delta$ -dodecalactone (Y)
5	menthol (+)	25	pulegone (R)	45	$\gamma$ -hexalactone (X)
6	menthol (-)	26	pulegone(S)	46	$\gamma$ -hexalactone (Y)
7	isobornyl acetate (X)	27	camphor (S)	47	$\gamma$ -eptalactone (X)
8	isobornyl acetate (Y)	28	camphor (R)	48	$\gamma$ -eptalactone (Y)
9	linalyl acetate (R)	29	rose oxide (4R4S cis)	49	$\gamma$ -octalactone (X)
10	linalyl acetate (S)	30	rose oxide (2S4R cis)	50	$\gamma$ -octalactone (Y)
11	cis 2-methyl-3.-hexenyl butyrate (X)	31	rose oxide (2R4R trans)	51	$\gamma$ -nonalactone (X)
12	cis 2-methyl-3.-hexenyl butyrate (Y)	32	rose oxide (2R4R trans)	52	$\gamma$ -nonalactone (Y)
13	hydroxycitronellal (X)	33	$\delta$ -hexalactone (X)	53	$\gamma$ -decalactone (X)
14	hydroxycitronellal (Y)	34	$\delta$ -hexalactone (Y)	54	$\gamma$ -decalactone (Y)
15	chrysanthemic acid (X)	35	$\delta$ -octalactone (X)	55	$\gamma$ -undecalactone (X)
16	chrysanthemic acid (Y)	36	$\delta$ -octalactone (Y)	56	$\gamma$ -undecalactone (Y)
17	2-phenylpropionic acid S)	37	$\delta$ -nonalactone (X)	57	$\gamma$ -dodecalactone (X)
18	2-phenylpropionic acid (R)	38	$\delta$ -nonalactone (Y)	58	$\gamma$ -dodecalactone (Y)
19	2-methylbutyric acid (S)	39	$\delta$ -decalactone (X)		
20	2-methylbutyric acid (R)	40	$\delta$ -decalactone (Y)		

353

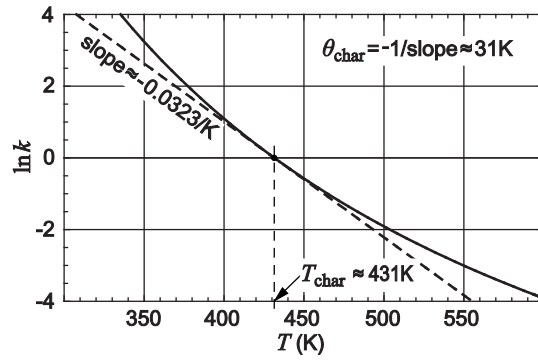
#	DA column				DE column				DM column				PEN column			
	$\Delta S$ , J/mol/K	$\Delta H$ , kJ/mol	$T_{char}$ , °C	$\theta_{char}$ , °C	$\Delta S$ , J/mol/K	$\Delta H$ , kJ/mol	$T_{char}$ , °C	$\theta_{char}$ , °C	$\Delta S$ , J/mol/K	$\Delta H$ , kJ/mol	$T_{char}$ , °C	$\theta_{char}$ , °C	$\Delta S$ , J/mol/K	$\Delta H$ , kJ/mol	$T_{char}$ , °C	$\theta_{char}$ , °C
1	171.2	65.7	94.5	17.10	181.3	69.6	94.9	16.19	144.8	58.5	110.7	20.94	131.2	51.6	98.6	22.26
2	175.2	67.3	94.7	16.73	185.8	71.2	95.0	15.83	148.3	59.8	110.5	20.46	132.8	52.2	98.5	22.00
3	143.3	60.8	129.6	22.19	169.4	69.6	120.1	18.48	143.2	62.6	142.1	22.89	133.9	58.2	137.8	24.14
4	143.3	60.8	129.6	22.19	171.3	70.3	119.9	18.27	144.4	63.1	141.9	22.71	133.9	58.2	137.8	24.14
5	143.6	64.1	150.4	23.29	161.8	70.7	144.4	20.49	139.7	66.1	175.6	25.32	150.5	68.8	161.7	22.86
6	148.2	66.0	150.4	22.60	163.8	71.5	144.1	20.24	140.4	66.4	175.7	25.21	151.6	69.2	161.7	22.70
7	104.5	48.9	162.9	32.33	116.6	53.3	155.6	28.69	112.4	53.9	176.4	31.15	116.5	54.5	165.8	29.39
8	104.5	48.9	162.9	32.33	118.0	53.8	155.2	28.34	113.8	54.6	176.1	30.75	117.8	55.0	165.6	29.08
9	129.7	57.7	146.8	25.43	132.0	58.8	148.0	25.08	125.8	58.8	168.0	27.50	116.9	53.8	159.1	28.86
10	131.8	58.5	146.1	25.00	135.1	60.0	147.5	24.50	126.4	59.1	167.9	27.36	116.9	53.8	159.1	28.86
11	138.1	60.6	142.4	23.71	141.3	62.3	145.4	23.37	126.8	59.0	166.1	27.17	134.2	60.5	153.3	25.00
12	139.8	61.2	142.0	23.42	143.8	63.3	145.1	22.96	128.4	59.7	165.9	26.84	135.5	61.0	153.1	24.77
13	160.8	75.9	177.2	22.23	161.1	72.5	156.5	21.17	142.9	69.1	186.0	25.36	130.7	62.4	178.3	27.13
14	160.9	76.0	178.0	22.26	162.4	73.0	156.3	21.00	144.0	69.6	185.9	25.17	130.7	62.4	178.3	27.13
15	123.4	58.1	170.7	28.18	153.6	70.8	166.2	22.65	148.9	71.8	185.6	24.36	138.1	66.8	185.2	26.15
16	123.4	58.2	170.8	28.16	162.1	74.6	166.3	21.53	150.1	72.4	185.6	24.18	145.0	70.1	185.8	24.99
17	145.7	70.2	184.9	24.84	167.4	80.1	184.4	21.74	161.9	80.8	203.4	23.37	145.2	73.2	205.8	26.05
18	151.1	72.6	184.6	23.98	171.5	82.0	184.8	21.26	164.1	81.8	203.0	23.05	148.4	74.7	205.7	25.51
19	192.3	80.1	127.7	16.67	183.8	76.0	123.9	17.25	140.3	62.0	146.1	23.56	145.7	62.7	136.0	22.19
20	192.6	80.3	127.8	16.65	185.0	76.5	124.3	17.16	141.4	62.5	146.2	23.40	148.7	64.0	136.5	21.79
21	103.9	40.6	90.8	27.13	146.4	57.3	99.1	20.10	118.9	50.2	123.7	26.09	118.5	48.2	109.1	25.20
22	106.6	41.5	90.4	26.46	147.2	57.7	99.2	19.99	125.3	52.8	123.8	24.83	121.6	49.4	109.4	24.61
23	106.3	44.3	115.9	28.40	130.7	54.7	122.2	23.76	120.3	53.3	143.9	27.11	122.6	52.5	130.0	25.75
24	106.3	44.3	115.9	28.40	135.5	56.7	123.1	23.02	125.0	55.4	144.3	26.17	124.5	53.3	130.4	25.39
25	105.8	49.3	161.4	31.86	132.1	59.8	154.9	25.47	129.5	61.6	175.9	27.22	129.0	60.0	165.9	26.71
26	105.8	49.3	161.4	31.86	134.4	60.8	154.8	25.06	132.7	62.9	175.3	26.57	131.4	61.0	165.6	26.23
27	115.6	51.3	142.9	28.07	126.7	55.1	137.3	25.41	116.6	54.1	162.7	29.17	112.8	51.6	155.1	29.58
28	121.2	53.6	142.8	26.84	130.1	56.5	137.0	24.75	119.0	55.2	162.5	28.60	112.8	51.6	155.1	29.58
29	128.1	54.4	127.7	24.56	135.5	57.7	129.9	23.42	116.9	53.4	155.5	28.63	126.8	55.4	138.7	25.48

30	129.2	54.8	127.5	24.34	136.8	58.2	130.0	23.20	120.4	55.0	156.2	27.88	128.8	56.1	138.5	25.09
31	129.1	55.1	130.1	24.53	136.7	58.5	132.4	23.36	114.6	52.7	158.1	29.35	120.1	53.5	145.8	27.28
32	130.0	55.5	129.9	24.34	138.6	59.3	132.3	23.05	114.6	52.7	158.1	29.35	120.1	53.5	145.8	27.28
33	182.2	85.8	178.9	19.80	162.7	71.1	144.3	20.37	144.1	67.2	169.8	24.28	111.8	51.7	159.4	30.11
34	187.4	88.3	179.6	19.30	164.7	71.9	144.0	20.13	145.8	68.0	170.0	24.02	111.8	51.7	159.4	30.11
35	154.2	73.9	183.7	23.48	138.6	64.4	167.3	25.03	131.4	64.3	189.2	27.65	138.4	65.7	176.9	25.62
36	159.2	76.3	184.3	22.80	141.5	65.7	167.4	24.56	134.3	65.6	189.4	27.09	139.6	66.2	176.7	25.41
37	153.9	75.3	192.9	23.98	137.2	65.3	177.8	25.88	134.5	67.3	200.1	27.69	121.0	60.4	196.3	30.33
38	157.1	76.8	193.0	23.53	138.6	65.9	177.5	25.62	136.4	68.2	200.1	27.32	121.0	60.4	196.3	30.33
39	143.7	72.1	203.7	26.21	142.4	69.3	188.5	25.58	132.3	67.9	211.9	28.81	126.2	64.4	208.0	29.90
40	147.0	73.7	203.7	25.64	144.0	69.9	188.1	25.30	133.9	68.6	211.8	28.49	126.2	64.4	208.0	29.90
41	146.1	74.8	213.4	26.32	147.7	73.2	198.4	25.24	137.0	71.6	222.1	28.48	124.9	65.3	219.6	30.92
42	149.7	76.5	213.1	25.70	149.2	73.9	198.1	24.99	138.8	72.5	221.8	28.11	124.9	65.3	219.6	30.92
43	145.0	75.9	224.4	27.10	135.7	69.9	214.7	28.30	141.9	75.4	231.5	28.06	129.7	69.1	230.2	30.47
44	147.9	77.3	224.2	26.58	136.4	70.2	214.5	28.15	143.7	76.3	231.1	27.71	129.7	69.1	230.2	30.47
45	168.9	79.0	174.2	21.07	138.8	60.5	140.2	23.48	131.5	60.8	163.7	26.10	125.7	56.2	148.4	26.28
46	176.9	82.9	176.4	20.25	145.7	63.6	141.9	22.51	136.5	63.2	165.1	25.28	128.0	57.2	148.6	25.85
47	170.6	80.3	177.5	21.03	140.6	62.9	151.6	23.83	130.1	61.7	174.9	27.06	128.2	59.2	162.8	26.69
48	173.5	81.7	178.0	20.71	147.9	66.2	152.6	22.76	133.9	63.5	175.7	26.36	131.0	60.4	163.0	26.17
49	168.5	80.8	185.4	21.65	141.5	65.1	163.1	24.33	133.5	64.9	186.6	27.10	134.7	63.8	175.1	26.20
50	171.9	82.4	185.8	21.26	148.7	68.3	163.6	23.22	136.9	66.5	187.0	26.48	137.2	64.9	175.1	25.73
51	159.8	78.4	195.1	23.26	133.7	63.5	175.9	26.42	138.3	68.7	197.7	26.82	134.3	65.4	187.7	27.00
52	163.3	80.0	195.2	22.79	139.5	66.1	175.9	25.37	141.9	70.4	197.8	26.20	136.7	66.5	187.5	26.55
53	156.6	78.7	206.5	24.29	131.0	64.3	191.1	27.85	131.6	67.8	213.8	29.07	139.4	69.4	198.9	26.69
54	159.7	80.3	206.6	23.83	134.6	66.0	191.1	27.15	134.7	69.3	213.5	28.43	141.7	70.4	198.6	26.27
55	167.0	84.8	212.4	23.11	136.8	68.4	200.3	27.25	138.4	72.1	220.3	28.09	137.2	70.1	211.0	27.79
56	169.5	86.0	212.6	22.80	140.4	70.1	200.2	26.58	141.0	73.3	220.2	27.59	139.5	71.2	210.5	27.32
57	165.0	85.6	222.7	23.89	134.7	69.0	212.1	28.35	143.3	75.9	229.8	27.70	142.2	74.0	221.0	27.42
58	167.7	86.9	222.6	23.51	137.4	70.3	211.8	27.81	144.8	77.2	229.5	27.21	144.6	75.1	220.3	26.96

355  
356

357 **Figures**

358 Figure 1:



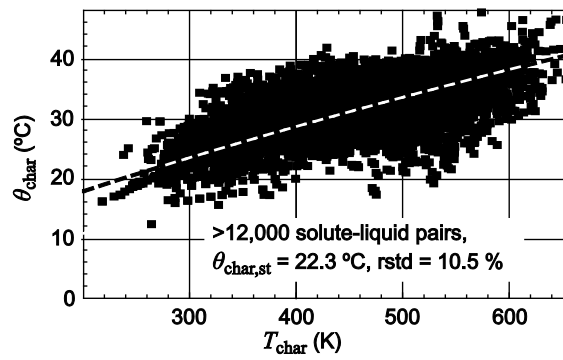
359

360

361

---

362 Figure 2:

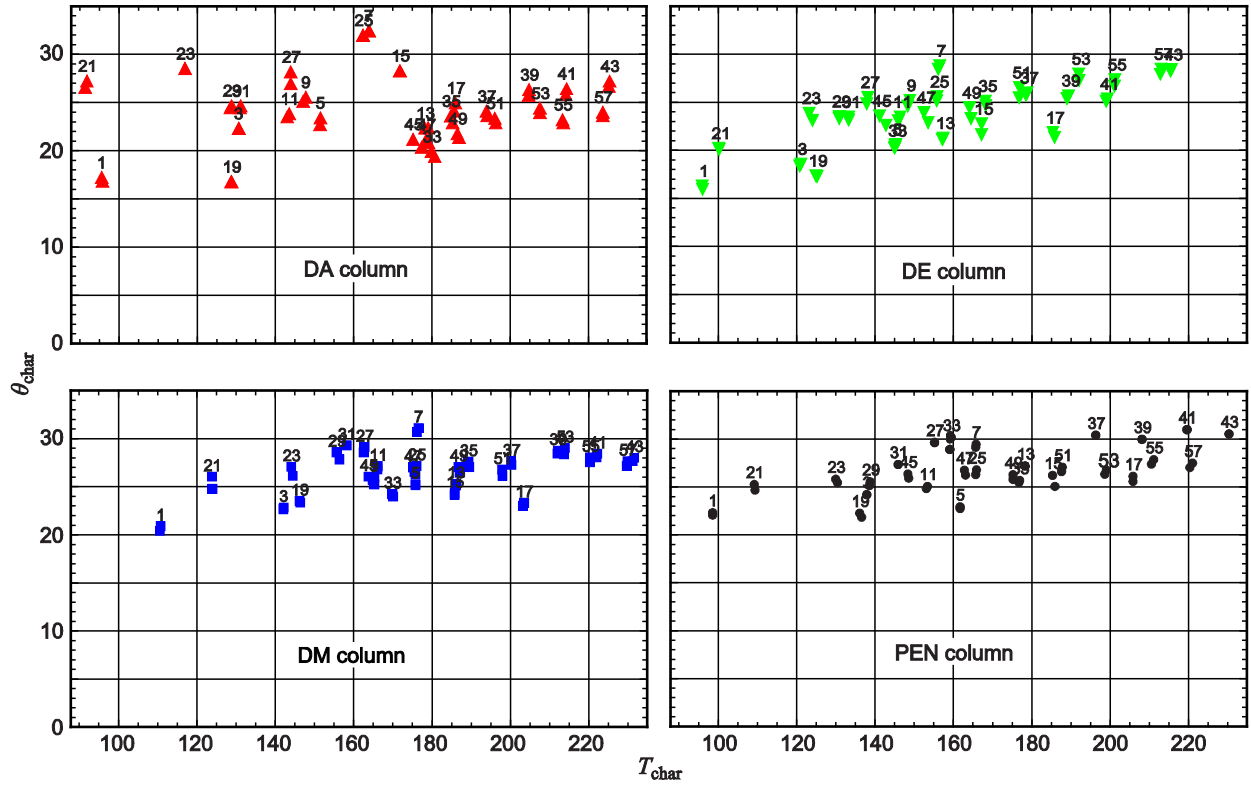


363

364

365



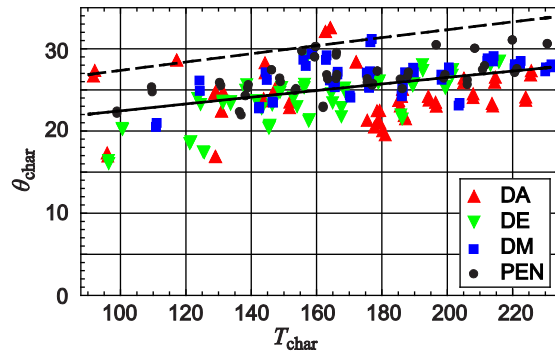


367

368

369

370 Figure 4



371

372